Int. J. Multiphase Flow, Vol. 1, pp. 793–816. Pergamon/Elsevier, 1975. Printed in Great Britain.

DROP TRAJECTORY PREDICTIONS AND THEIR IMPORTANCE IN THE DESIGN OF SPRAY DRYERS

W. H. GAUVIN, S. KATTA and F. H. KNELMAN*

Department of Chemical Engineering, McGill University, Montreal, Quebec, Canada

(*Received* 23 *March* 1974)

Abstract—A knowledge of the trajectories of atomized droplets in both the nozzle zone (where the droplets are rapidly decelerating from their initial high velocity) and in the free-entrainment zone (where the droplets are conveyed by the drying gas) is required for the design of spray dryers, since it governs the evaporative capacity and thermal efficiency of the chamber, while affecting the moisture content and general quality of the product through the control of the drying time.

The trajectories of droplets in three-dimensional motion were determined theoretically in both zones. In the case of two-fluid pneumatic atomizers, the characteristics of the jet of atomizing fluid were found to be important in both the zones.

Predictions of droplet trajectories were tested in an experimental circular cocurrent spray-drying chamber with a conical bottom, in which the drying air was introduced tangentially near the top. Water was used as the feed material. A study was made of the effects of liquid feed rate and temperature, drying air flowrate and temperature, and of nozzle position on the thermal efficiency and evaporative capacity of the chamber. The results were interpreted in the light of the droplet trajectories predicted.

INTRODUCTION

A knowledge of the trajectories of vaporizing droplets is required in the design of a number of industrial applications, such as spray coolers and absorbers, cyclone evaporators, venturi scrubbers and combustion devices involving sprays of liquid fuels. Such a knowledge is particularly important in spray drying, since it governs not only the evaporative capacity of a given drying chamber, but also the properties and quality of the spray-dried product obtained from it. In spite of a large body of published experimental data, this particular aspect of the theory of spray drying has remained largely unexplored. The few attempts published in the past, as summarized, for example, by Masters (1972) were based on unrealistic, highly simplified models.

The objective of the present study was to predict the droplet trajectory in the nozzle zone (defined as the range of particle motion traversed by the droplets as they rapidly decelerate from their high initial velocity as they emerge from the atomizing nozzle and terminating when the unevaporated droplets begin to be entrained by the swirling drying gas) and in the free-entrainment zone (where the droplets are freely-conveyed by the drying gas) which will permit a better understanding of the effect of various factors on the capacity and thermal efficiency of a spray drying chamber.

A critical review of the work published in the field of spray drying until 1967 has been presented by Baltas & Gauvin (1969a, b). An attempt will now be made to review the more

* Present address: Department of the Humanities of Science, Sir George Williams University, Montreal, P.Q.

recent work while recalling some important investigations carried out in the past which are particularly pertinent to the present study.

Edeling (1949) was one of the first to attempt an analysis of the flow pattern and droplet trajectories in a cylindrical spray dryer based on a simplified approach. Manning & Gauvin (1960) measured the evaporation rates of a spray in the nozzle zone and found that the heat transfer correlation proposed by Ranz & Marshall (1952) was applicable despite the high deceleration of the drops and the complex flow present near the nozzle. Their experimental measurements of air velocity, air temperature and droplet velocities within the spray are particularly pertinent to the prediction of the droplet trajectories in the nozzle zone. As far as the free-entrainment zone is concerned, Dlouhy & Gauvin (1960) found that the individual droplets in this zone evaporated at a rate corresponding to stagnant conditions, that is, with a Nusselt number equal to 2. They also observed that the presence of the droplets as a cloud had no influence on the rate of evaporation of an individual droplet. Finally, they showed that the progressive evaporation in a downward, cocurrent cylindrical spray dryer could be predicted by dividing the spray into a small number of drop size groups and carrying out the stepwise calculations over a small increment of time.

Baltas & Gauvin (1969a) developed a more accurate, but more complex, stepwise prediction procedure that took into account the radial gradients present in the spray and the radial mixing. Applications of their approach to the case of the evaporation and drying of a sodium nitrate solution in a downward cocurrent spray dryer was only partially successful, owing to the uncertainties of the behaviour in the nozzle zone. In a second paper (1969b), they investigated the characteristics of the same spray dryer, and found that the axial injection of the spray increased the radial turbulent diffusivity of the air stream which enhanced the radial mixing. Steep radial gradients in the spatial density of the spray were shown to exist even at a considerable distance from the atomizer.

Pita (1969) conducted a study on the cooling of water sprays in the open atmosphere. He obtained empirical correlations to predict the heat transfer rates from conical and flat sprays to the atmosphere. He confirmed that the drop size distribution in heat and mass transfer phenomena could be represented by D_{vs} and presented an approximate equation of limited applicability to predict the residence time of a droplet in the nozzle range. Bailey *et al.* (1970) presented solutions for trajectories of evaporating particles for some specific cases in an idealized two-dimensional flow field. Their analysis is valuable as they considered the effect of Spalding number to take into account the effect of heat transfer on mass transfer under high temperature conditions.

Kim & Marshall (1971) studied the atomizing characteristics of pneumatic nozzles by a novel technique of spray-cooling molten wax and melts of wax-polyethylene mixtures to obtain drop size distributions at the nozzle exit, thus avoiding the effects of evaporation in the nozzle zone on the droplet size distribution. They presented correlations for a wide range of operating variables, the most important of which they showed to be the dynamic force of the atomizing gas, $V_{\mathrm{rel}}^2\rho_a$, and the ratio of mass flowrates of air to liquid. In general, according to these authors, a mean spray size can be expressed as follows:

$$D_{vs} = A/(V_{\mathrm{rel}}^2\rho_a)^{\alpha} + B(W_a/W_L)^{\beta} \qquad [1]$$

where α and β are functions of nozzle design and A and B are functions of both nozzle design and liquid properties.

Hoffman & Ross (1972) found theoretically that the effect of mass transfer on heat transfer to an evaporating droplet is to cause a decrease, the relative decrease being independent of the Re and being a function only of the Spalding number B in the Re range 0–500.

The success of the prediction of the droplet trajectories in spray drying depends on the knowledge of the flow patterns in the different regions of the spray chamber, and the accuracy of the value of the drag coefficient to be used in the equations of motion, in addition to the validity of the heat and mass transfer correlations for predicting the decrease in droplet diameter during evaporation.

Prediction of the flow pattern in the nozzle zone is difficult due to the presence of the strong induction effects exerted by the expanding spray. The situation is particularly complex in cylindrical or conical chambers with tangential air inlets. Numerous studies on the flow of jets were reported in the past. Albertson *et al.* (1950) carried out an extensive investigation on the properties of free air jets, and reported measurements of both the longitudinal and radial velocities. Their results are of particular interest since they measured the axial velocities far from the nozzle exit (up to 250 nozzle diameters) and since very few investigators have investigated the radial velocities of a jet.

Recently Gal (1970) analyzed the results of several investigations on compressible and incompressible jets, under both isothermal and nonisothermal conditions. He presented the following correlation for the dimensionless centre-line velocity:

$$V_c/V_o = 6.5/\bar{x} \qquad [2]$$

where

$$\bar{x} = (\rho_a/\rho_0)^{1/2}(x/D_0). \qquad [3]$$

Gauntner *et al.* (1970) presented a brief survey on the properties of jets, including the variation of static pressure and turbulence distribution along the centreline of a free jet. Davies (1972) reported that for a free jet, the mass flow rate of entrainment M_e of surrounding gas experimentally measured is given by the following empirical relation:

$$M_e = M_0\{0.23(x/D_0) - 1\}. \qquad [4]$$

On the basis of conservation of momentum, Davies derived theoretically a similar equation with the numerical coefficient of 0.36 instead of 0.23. From the assumptions made in the derivation, it is expected that the coefficient of 0.36 will only hold in the zone immediately adjacent to the nozzle exit. Beyond two nozzle diameters, [4] is useful in the establishment of material and heat balances in the spray from which the temperature of the gas within the spray can be obtained.

Abramovich (1963) derived equations to determine the variation of the axial velocity and of the concentration along the centreline for a two-phase jet of air with an admixture of solid particles or droplets, on the basis of total momentum conservation. Although this approach is not strictly applicable to the case of evaporating droplets in a jet, it is of interest

to note that, for equal mass flowrates of air and of solid particles, the variation of gas velocity along the centreline is close to that of a single-phase isothermal air jet and the difference would even be less in the case of an evaporating spray.

So far, only rectilinear, cocurrent flows have been considered. Many modern spray dryers are, however, of the swirl or vortex type. The advantages of a centrifugal field are that it increases the droplet residence time and tends to stabilize the flow pattern. Very little information is, however, available on the latter. The most pertinent study is probably that of Schowalter & Johnstone (1960) who investigated the axial and tangential velocities, as well as the structure of turbulence, in a 20.3-cm i.d. pipe approximately 152 cm long. The air entered tangentially through an involute entry at one end, and left at the opposite open end. They found that the spiralling flow was not symmetrical about the axis of the pipe. Their results indicate that the flow only made approximately three turns before exiting from the pipe. The flow in the central portion of the pipe was of nearly constant angular velocity over slightly less than one-half of the radius. Axial velocities increased sharply towards the wall. The same behaviour was observed with tangential velocities which, for an entrance velocity of 30.5 m/s decreased from values above 27 m/s near the entrance (the maximum value in a given plane, recorded about 2.54 cm from the wall) to about 24 m/s near the exit. The longitudinal intensity of turbulence increased sharply near the centre (to about 15%), and so did the radial intensity (to about the same value), but this can be ascribed largely to the abrupt decrease in mean velocity near the centre. This study indicated that the flow pattern was not sensitive to changes in inlet velocities, but was probably very sensitive to the geometry of the system and particularly to the design of the inlet conditions. For this reason, the conclusions to be drawn from this work are only of a qualitative nature. Place *et al.* (1959) have shown the complexity of flow patterns in a spray dryer with swirling flow. An important conclusion from their work, however, was that the spray exerted very little effect on the flow pattern of the surrounding drying gas. Quite recently, Lewellen (1971) has presented a critical review of the theoretical and experimental evidence available on confined vortex flows. Although excellent from the point of view of background information, this review does not permit a prediction of the flow patterns in a spray drying chamber.

The first part of the present paper deals with the flow patterns and the predictions of the trajectory of the largest droplet in both the nozzle zone (where the droplets are rapidly decelerating from their initial high velocity, with relative Reynolds numbers ranging from 80 down to 0.1), and in the free-entrainment zone of a spray-drying chamber with tangential air entry (where the droplets are conveyed by the drying gas, with relative Reynolds numbers from zero to 0.1). The second part is devoted to a study of the effects of a number of operating parameters on the thermal efficiency and evaporative capacity of the chamber. The experimental data obtained under non-adiabatic conditions simulating commercial operation were interpreted in the light of droplet trajectories.

EXPERIMENTAL

For the present study, water only was used as feed material. For each set of operating conditions, the maximum evaporative capacity of the chamber was determined. A choice

of two criteria was available for the determination of this maximum capacity: (a) that no droplets of water should leave unevaporated in the exit gas; or (b) that no droplet should hit the walls of the chamber. The latter was selected as being the more exacting criterion on the basis of experimental observation.

Equipment

The experimental installation consisted briefly of a direct gas-fired furnace connected to a motor-blower assembly, which provided the required drying air; the spray-drying chamber proper, a cocurrent down flow type with tangential air entry; the feed system, consisting of a pneumatic nozzle assembly, feed tank and pump; and the collection unit, a multicone-type cyclone collector, which was used in subsequent studies on the drying of aqueous solutions, but was retained in the present work because it provided a convenient metering device for the determination of the volumetric flow-rate.

The chamber was constructed of 0.015-cm thick galvanized steel and consisted of two main sections, an upper jacketed cylindrical section, 1.22-m i.d. × 0.61-m high, and a 50.23° lower conical section, 1.22-m high (0.076-m diameter at the bottom), the bottom part of which could be removed to permit entry to the chamber.

The hot air from the blower was introduced tangentially into a 5.1-cm wide annular jacket surrounding the cylindrical section, distribution to the chamber proper being provided by six 3.8-cm × 15.2-cm slots cut in the inside wall at an angle of 45°. The metal was not cut out, but merely bent back along a 90-degree edge to force the air flow to assume a fairly tight spiral pattern. All protruding joints were in the air jacket, leaving the drying chamber quite smooth. The entire chamber and entering ducts were coated internally with a high-temperature aluminum paint and heavily covered externally with an insulating material called "Tartan" cement. Heat losses were determined from data supplied by the manufacturers; they checked quite well against losses calculated from a heat balance. The bottom of the drying chamber was connected to a small commercial Aerotec multicone collector, consisting of five parallel banks of five 5.1-cm cyclone tubes each. The spent gases were exhausted to the outside. The volumetric rate of flow of the drying air was calculated from pressure drop measurements across the Aerotec unit, which had been previously calibrated by means of Pitot tube traverses in the 20.3-cm inlet duct. The values reported in this study include the small amount of compressed air to the nozzle.

Characteristics of atomizing nozzle

An internal-mixing two-fluid nozzle (Spraying Systems Co., type 22-B, orifice diameter = 0.356-cm) was used exlusively. The pressure of the atomizing air was precisely controlled by a needle valve and its flow rate was measured by an orifice. Provision was made to adjust the position of the nozzle at any predetermined level in the chamber.

The droplet size distribution and mean Sauter diameter, D_{vs}, produced by this nozzle were determined as a function of the atomizing air pressure and feed water temperature, respectively. The measurements were carried in water-saturated drying air, to minimize spray evaporation. Spray samples were collected in Varsol-filled optical cells of the type described by Dlouhy & Gauvin (1960) and the drops were measured microscopically.

Many of the tests were conducted with an atomizing air pressure of 44.6 N/cm^2 and a feed water temperature of 285 K. Under these conditions, the drop size distribution was as follows:

Drop diameter (μm)	3.8	10	16	24	30	37	44
Frequency (%)	3	16	28.4	29.2	15.2	6	1.4

The maximum observed drop diameter was in the range 62–65 μm (it was slightly over 100 μm for an atomizing air pressure of 21.2 N/cm^2 and a feed water temperature of 285 K). The angle of the spray varied only slightly with the rate of feed water to the nozzle and remained nearly constant at 22°.

Procedure

To determine the maximum capacity of the chamber, under a given set of operating conditions when steady state was reached, the feed rate was increased very slowly, until droplets began to hit the wall. Owing to the special observation and lighting facilities provided in the equipment, any droplet hitting the walls or the side observation windows could be easily detected as a tiny flash or pinpoint of light. The feed was then slowly reduced until this effect just disappeared and all pressures, temperatures and flow rates were recorded at that point. It was observed that the maximum rate of feed was quite reproducible.

1. DROPLET TRAJECTORY

Exact calculation of the trajectory of a droplet in a centrifugal flow field requires the simultaneous solutions of a series of equations to express (i) the three-dimensional motion of the droplet; (ii) the instantaneous rate of evaporation of the droplet, and hence its diameter at time t; (iii) the instantaneous three-dimensional flow pattern of the drying gas; and (iv) the instantaneous properties (temperature, humidity and heat capacity) of the latter. These equations will now be developed for the purpose of calculating the trajectory of the droplet of maximum experimentally-observed size (65 μm) produced by the nozzle used in this study.

Equations of motion

The equation of motion of a droplet in centrifugal and gravitational fields can be written as:

$$dV_f/dt = g + r\omega^2 + V_t V_r/r - C_D V_f^2 \rho_a A_p/2m + F_L/m \qquad [5]$$

where the terms on the right side are due to the gravitational, centrifugal, Coriolis, drag and lift forces, respectively. The buoyancy force, added mass, pressure gradient and Basset-history terms have been neglected as being several orders of magnitude too small (Hinze 1959). Realizing that the drag force acts opposite to the resultant of the external forces while

the lift force acts radially, the droplet velocities in the three-dimensions can be expressed as follows:

$$dV_t/dt = -V_tV_r/r - 3C_D\rho_aV_f(V_t - V_{at})/4D\rho \quad [6]$$

$$dV_r/dt = V_t^2/r - 3C_D\rho_aV_f(V_r - V_{ar})/4D\rho + F_L/m \quad [7]$$

$$dV_v/dt = g - 3C_D\rho_aV_f(V_v - V_{av})/4D\rho \quad [8]$$

where V_f, the actual velocity of the droplet in its path relative to the fluid, is given by:

$$V_f^2 = (V_t - V_{at})^2 + (V_v - V_{av})^2 + (V_r - V_{ar})^2. \quad [9]$$

The drag coefficient was evaluated by means of the following equations proposed by Beard & Pruppacher (1969) for different ranges of Re:

$$C_D = 24/Re \qquad Re < 0.2 \quad [10]$$

$$C_D = (24/Re)(1.0 + 0.1Re^{0.99}) \qquad 0.2 < Re < 2 \quad [11]$$

$$C_D = (24/Re)(1.0 + 0.11Re^{0.81}) \qquad 2 < Re < 21 \quad [12]$$

$$C_D = (24/Re)(1.0 + 0.189Re^{0.632}) \qquad 21 < Re < 200. \quad [13]$$

In a general way, the lift force on a droplet can be shown to be due to its spin and also to the shear force acting on it (Lawler & Lu 1970). However, the spin component was estimated to be negligible in the present study. Saffman (1965) obtained the following equation for a shear lift force on the motion of a sphere in an unbounded shear flow:*

$$F_L = 20.25\rho_aD^2(v/K)^{0.5}KV_f/g_c \quad [14]$$

where K is the curl of the fluid velocity. K is given by:

$$K = -dV_{av}/dr. \quad [15]$$

This can be shown to be equivalent to

$$K = 1.4V_{av}(r/r_5^2) \quad [16]$$

when the axial jet velocities are estimated as a function of their distance from the centreline from the following equation (Pai 1954):

$$V_{av} = V_c \exp[-0.692(r/r_5)^2]. \quad [17]$$

Lawler & Lu (1970) confirmed the form of equation [14] for the radial migration of particles in pipe flow. For the present study, Saffman's equation was used to estimate the lift force acting on the droplet when the droplet Re was less than one, and assumed to be negligible, in comparison to the magnitude of other forces, at higher Reynolds numbers.

Droplet evaporation rate

The change in diameter of the droplet is given by:

$$\lambda_w \cdot d(\pi\rho D^3/6)/dt = h\pi D^2(t_a - t_w). \quad [18]$$

* The coefficient in equation [14] is not known exactly for the conditions prevailing in the present study and hence Saffman's value of 20.25, which was derived theoretically, was used. However, the effect of the lift force was found to be negligibly small for droplet sizes considered here.

Hence:

$$dD/dt = 2h(t_a - t_w)/\lambda_w \cdot \rho. \quad [19]$$

These equations assume that the droplets are at the wet bulb temperature of the drying air. Lyons (1951) has shown experimentally that this is indeed so, even in the nozzle zone, at a short distance (0.32 cm) from the nozzle exit. For the large droplet, h was determined from the correlation proposed by Ranz & Marshall (1952), which, for air, takes the form:

$$Nu = 2.0 + 0.525(Re)^{0.5}. \quad [20]$$

For other droplets of smaller diameter in the distribution, h was calculated on the assumption that Nu is equal to 2. This was confirmed by Dlouhy & Gauvin (1960) for evaporating water sprays. This assumption eliminated the need to obtain the trajectories of all the droplets.

The change in size, for different classes of droplets, can be followed by:

$$dD_i/dt = 4k_a(t_a - t_w)/(D_i\lambda_w\rho). \quad [21]$$

Hence, the rate of heat transfer for the whole cloud of droplets is given by the following equation:

$$dq/dt = 2\pi k_a(t_a - t_w)\sum n_i D_i \quad [22]$$

where n_i is the number of droplets of size D_i.

Gas flow patterns

The flow field in the spray chamber is very complex and, due to lack of information on the interaction of a vortex flow on a jet, it was assumed that the flow behaved as a superposition of the jet of atomizing fluid and the surrounding centrifugal field of the drying air. This is justified in view of the finding of Becker *et al.* (1963) who observed that, in the case of a turbulent jet issuing axially into a cylindrical chamber fed by a uniform stream, the flow acted as the superposition of both the streams.

An important parameter describing the flow of a jet is the velocity half-radius which has been shown to be a linear function of the distance x from the nozzle exit (Abramovich 1963). There is conflicting evidence on this variation in the literature (Hinze 1959; Gauntner *et al.* 1970). After examining the results of several investigations, a coefficient of 0.09 in the following equation was chosen:

$$r_5 = 0.09x. \quad [23]$$

The centreline velocities were computed from the equations of Gal (1970), which were given earlier [2] and [3]. The variation of the axial velocity with radius is given by [17]. The radial velocities reported by Albertson *et al.* (1950) were fitted by the following 2nd order polynomial which was used in the computations:

$$V_{ar} = [-35.6(r/x)^2 + 5.7(r/x) + 0.1]D_0V_0/x. \quad [24]$$

In the entrainment zone, the axial gas velocities were obtained by adding the axial velocities in the main flow field and the velocities in a jetting flow as predicted from the equations given earlier. Vertical air velocities were calculated, including the water vapor, on the basis of total volumetric flow at any section in the chamber, assuming that these values remained constant along the horizontal plane. The tangential air velocities were determined experimentally by means of a Pitot tube with a spherical head. Considerable difficulty was experienced close to the chamber axis because of both the high drop density and the low gas velocity in that region. Typical results of traverses at three different levels are given in table 1. These results show that there are two zones in the vortex flow, a central zone and an annular zone near the wall, in which V_{at} was found to vary according to the two following equations, respectively:

$$V_{at} = C_1 \cdot r \qquad [25]$$

$$V_{at} = C_2(R - r) \qquad [26]$$

where C_1 was a function of the axial distance from the nozzle and C_2 remained constant. Tangential gas velocities at other levels were obtained by means of linear interpolation.

Properties of drying gas

The temperature and humidity of the drying air at any point in the path of the droplet trajectory, and hence its other properties, can be estimated from the energy balance and the amount of feed evaporated up to that point. For the purpose of estimating t_a at a position z in the nozzle zone, entrainment from the surrounding drying gas must be taken into consideration. An energy balance in this zone taken over the wet bulb temperature of the drying air t_w yields the following equation:

$$(t_a - t_w) = \{M_e C_{s1}(t_{a1} - t_w) + W_L(t_f - t_w) - [(M_e + M_0)(H_z - H_1)\lambda_w]\}/[(M_e + M_0)C_{sz}] \qquad [27]$$

from which the temperature of air within the spray can be calculated. In obtaining the above equation, the heat losses were neglected and t_a was assumed constant at any plane. The rate of entrainment at any section of the jet was estimated from [4].

The humidity change in the air in the spray was estimated from the equation:

$$H_z = E_z/(M_e + M_0) + H_1. \qquad [28]$$

After a certain distance from the nozzle exit, the entrainment of inlet drying air would be complete and then M_e would become equal to the flowrate of the drying air. The amount of feed evaporated E_z was calculated purely on the basis of heat transfer to the droplets from the drying medium.

The viscosity and thermal conductivity of air were determined from the following equations reported by Hilsenrath *et al.* (1955):

$$\mu_a = 1.55 \times 10^{-6} t_a^{1.5}/(110.4 + t_a) \qquad [29]$$

$$k_a = 0.2646 \times 10^{-2} \sqrt{t_a}/[1 + (254.4 \times 10^{-12/t_a}/t_a)] \qquad [30]$$

where t_a is in K, μ_a is in N.s./m^2 and k_a is in J/m.s.K.

In the free-entrainment zone, the temperature of the air at any distance z measured along the path of the droplets was obtained from the following overall heat balance:

$$W_G(t_1 - t_w)C_{s1} + W_L(t_f - t_w) = W_G(t_a - t_w)C_{sz} + E_z\lambda_w + q_{Lz}. \quad [31]$$

It was assumed that the heat losses q_{Lz} were proportional to the evaporation which had occurred up to point z and that no radial gradients existed in the temperature of the drying air.

Method of calculations

According to the criterion selected for this study, the maximum evaporative capacity of a spray drying chamber (kg of water evaporated per hour) for a given set of operating conditions (chamber geometry, nozzle position and operating characteristics, and temperature, humidity and volumetric flow rate of entering drying air) is dictated by the requirement that the largest droplet on the edge of the spray at the end of the nozzle zone will be completely evaporated before it reaches the chamber wall. Whether this criterion is met for a given set of operating conditions can now be determined by the numerical solution of the equations of motion of the largest droplet, simultaneously with the equations for its instantaneous size, as developed in the previous sections. A computer program was written to handle the computations on an IBM 360/75 computer. The calculations were carried out over small increments of time (10^{-4} s initially, and 10^{-3} s for most of the calculations).

Results

As an illustration, calculations were carried out for an experimental run for which the operating conditions were as follows:

Mass flow rate of drying air (W_G)	= 500 kg/h
Temperature of inlet drying air (t_1)	= 489 K
Humidity of inlet drying air (H_1)	= 0.004 g of water vapor/g of dry air
Water feed temperature (t_f)	= 285 K
Mass flowrate of atomizing air (M_0)	= 32 kg/h
Atomizing air pressure	= 44.6 N/cm^2
Nozzle position below roof	= 27.3 cm
Heat losses	= 1200 J/s.

Under these operating conditions, the maximum evaporative capacity was experimentally determined to be 23.6 kg/h of water. (Other data collected were as follows: C_{s1} = 1068 J/kg K; t_2 = 372 K; H_2 = 0.049; C_{s2} = 1160; t_w = 326 K; λ_w = 2.376 J/kg.) The size distribution was given earlier, and the largest droplet was 65 μm. Finally, the tangential air velocities experimentally measured are given in table 1.

Table 1. Tangential air velocities, m/s

	Distance from wall (cm)						
x (cm)	3.0	6.1	9.1	12.2	15.2	18.3	24.4
46.3	2.2	2.6	—	2.4	—	2.0	1.8
76.8	2.4	2.5	2.2	2.1	1.9	1.8	1.3
125.0	3.0	3.0	2.0	1.3	—	—	—

The initial conditions for the nozzle zone were chosen to correspond to the data of Manning & Gauvin (1960) who measured droplet velocities issuing from an identical nozzle at a distance of 3.8 cm from the nozzle exit. For a 65-μm droplet on the edge of the spray these initial conditions were: $V_v = 55.5$ and $V_r = 9.8$ m/s (corresponding to a V_0 of approximately 366 m/s). An idea of the rapidity of drop deceleration can be gained from the fact that 30.5 cm below the nozzle, a 65-μm droplet is down to a velocity of 3 m/s.

In the nozzle zone, which extended a distance of about 76 cm below the nozzle as experimentally observed, Re decreased from an initial value of 80 down to 0.1. The computed amount of evaporation in this zone and the temperature change of the drying air are shown in figure 1. The increase in the latter during the first 0.01 s is due to entrainment effects. It is of interest to note that most of the evaporation and, hence, most of the change in drying air temperature takes place in the nozzle zone. The radial position of the droplet at the end of the nozzle zone was calculated to be close to 12.7 cm. The changes in computed V_v, V_r and V_f with time in the nozzle zone are shown in figure 2.

In the free-entrainment zone, the relative Reynolds number of the largest droplet varies between 0.1 initially and a final value of about zero. It enters this zone with a diameter of 38 μm, at a distance of 12.7 cm from the axis and 76.2 cm below the nozzle (or 103.5 cm below the roof of the chamber) that is, well within the conical section.

The change in diameter and position of the 65-μm (initially) droplet with time, in the entrainment zone, is shown in figure 3. The residence time of the droplet in this zone is about 0.4 s. Its trajectory indicates that it evaporated completely before it had a chance to

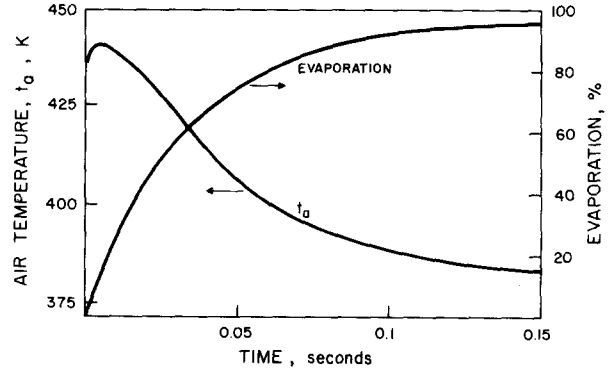

Figure 1. Evaporation and air temperature variations in nozzle zone.

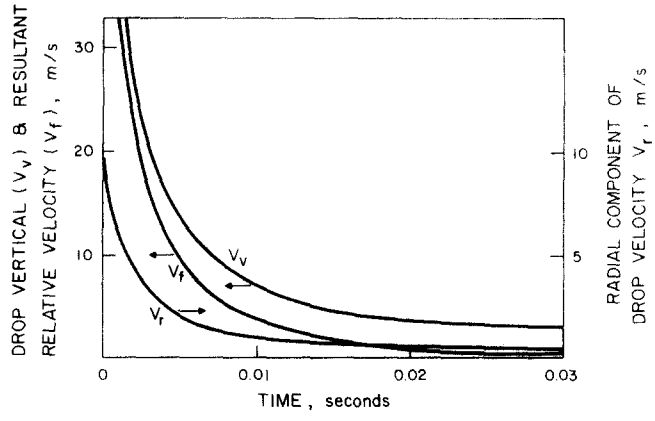

Figure 2. Variations in components of air velocity in nozzle zone.

come into contact with the wall which, at that point in time was still 6.1 cm away. This is in agreement with the experimental observations and confirms that the maximum capacity of the chamber was reached. A higher feed rate would have decreased the rate of heat transfer (because of the lowering in air temperature) and required a larger droplet path. To corroborate this result, calculations were repeated for a droplet initially 70 μm in diameter. Its change in diameter, also plotted in figure 3 indicates that it will not completely evaporate in its trajectory and that it will hit the wall when its diameter is still 14 μm.

The tangential and vertical components of the droplet velocity as a function of time are shown in figure 4. The increase in tangential velocity of the droplet with time is due to the fact that the tangential gas velocity increases with distance from the axis. After reaching the maximum value, V_t decreases with time since the droplet enters the annular zone where V_{at}, the absolute tangential velocity of the drying air, decreases steeply towards the wall.

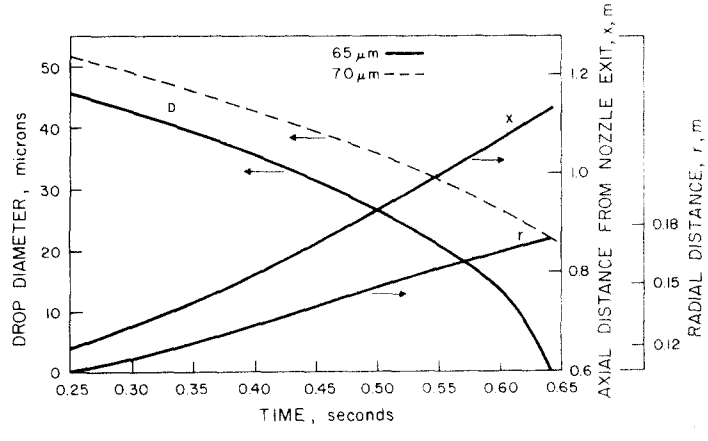

Figure 3. Variations in drop diameter and position in free-entrainment zone.

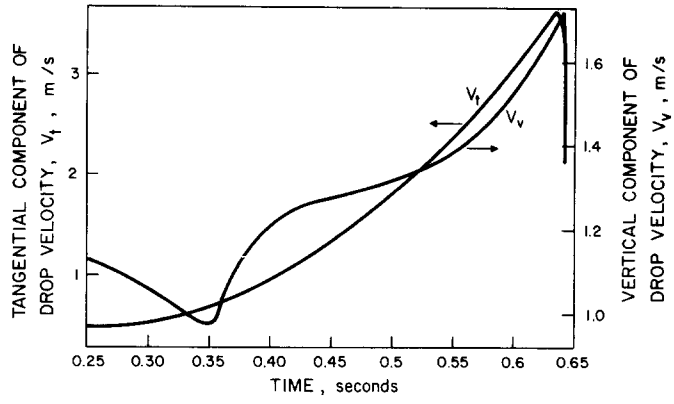

Figure 4. Tangential and vertical components of drop velocity in free-entrainment zone.

The initial behaviour of the vertical component of the droplet velocity is due to the interaction with the downward velocity of the jet and its subsequent gradual increase is due to the converging flow field in the conical section of the spray dryer. The radial velocity remained fairly constant.

Figure 5 shows the angular position of the droplet as a function of time. The droplet moved over an angle of 300° from its initial position until it disappeared. It is of interest to note that computations for the 70-μm droplet (initially) indicated that this larger drop moved over an angle of 325° before it hit the wall. However, major differences existed in the axial and radial positions of the two droplets.

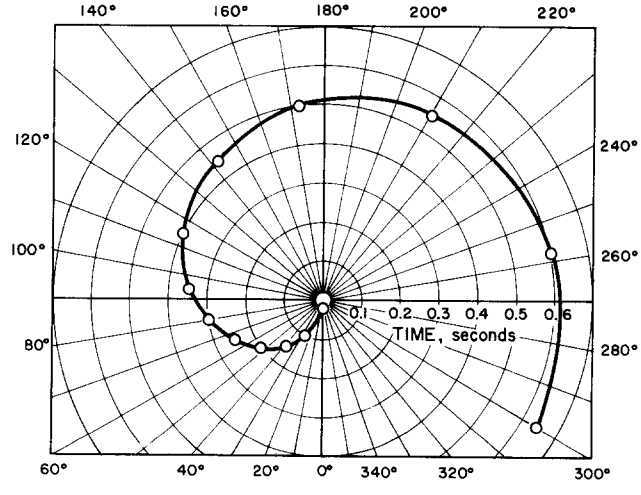

Figure 5. Angular position of droplet as a function of time.

2. SPRAY DRYING EFFICIENCY AND CAPACITY

Theoretically, the efficiency of a spray dryer will depend on the extent to which the outlet drying gas approaches a condition of equilibrium with respect to the water vapor pressure of the material being dried at the chamber exit. As long as the latter is greater than the existing pressure in the surrounding medium, water vapor will continue to diffuse from the material. In addition to all the factors which affect the drying path (geometry of the chamber, type and location of the atomizer, spray pattern, air flow patterns and velocity), the efficiency will also be affected by the factors which enter into the heat and mass transfer considerations (temperature of drying gas and of feed solution, droplet size distribution, water vapor pressure of drying material, extent of falling-rate period, if any) and also by external heat losses from the chamber.

Adequate attention has not been given to the efficiency of spray drying in the literature, and the various opinions which have been expressed concerning the performance of various spray-drying systems are frequently conflicting. It is believed that a chamber thermal efficiency based on the ratio of the heat used in vaporization to the total heat available would establish a firm basis for comparison of chamber performance.

An energy balance over any temperature datum t_d is given by:

$$W_G(t_1 - t_d)(C_{s1}) + W_L(t_f - t_d) = W_G(t_2 - t_d)(C_{s2}) + W_L\lambda_d + q_L. \quad [32]$$

For maximum efficiency, $q_L = 0$ and $t_2 = t_s = t_w$, and if the wet-bulb temperature of the air, t_w, is taken as the datum, the above equation simplifies to:

$$W_G(t_1 - t_w)(C_{s1}) + W_L(t_f - t_w) = W_L\lambda_w. \quad [33]$$

It is obvious that the corresponding efficiency term is:

$$\eta = W_L\lambda_w/[W_G(t_1 - t_w)C_{s1} + W_L(t_f - t_w)] \quad [34]$$

which will be called the *drying thermal efficiency*. Its maximum value is 100%, based on the equality indicated in [33].

For the purpose of this study, the capacity of a spray-drying chamber is simply measured as the kilograms of water evaporated per hour. For the purpose of comparison with other systems, it could equally well be expressed as kg water/(h) (m^3 of chamber). As stated before, the *maximum capacity* for a given set of operating conditions has been defined on the basis of the criterion that no droplets should hit the wall. This criterion is perhaps unduly harsh since in practice many industrial installations are operated under conditions which allow wet particles to hit the wall and continue to dry *in situ*. It was adopted in this work because of its relevance to the calculation of particle trajectories and because of its ease of experimental determination and excellent reproducibility.

In the results reported below, the maximum evaporative capacity and the corresponding thermal efficiency calculated from [34] are given for each set of operating conditions. By the process of progressive selection, the latter are successively so chosen as to lead to an optimum set of operating conditions. No effort was, however, made to optimize the design of the air inlets, as the profound influence exerted by the air entrance geometry

on the performance of the chamber was not fully appreciated until after the study had been completed.*

Effect of atomizing air pressure

Increasing the pressure of the atomizing air to the nozzle, besides decreasing the value of D_{vs}, also narrows the drop size distribution. More specifically, it decreases the number of the larger drops and also the maximum value of the diameter at which they can exist. A preliminary study was therefore made to ascertain the effect of the atomizing air pressure on the chamber capacity. The pressure of the atomizing air to the nozzle was varied from 18.4 to 44.6 N/cm^2, all other operating conditions being kept constant. This study showed rather strikingly the effect of the larger drop diameters on the capacity since, even though the variations in D_{vs} were rather small (from 26 to 32 μm), the capacity was reduced by more than one half when the atomizing pressure was dropped from 44.6 to 18.4 N/cm^2. The effect of the size of the largest droplet on the capacity has been clearly shown in Section 1 by comparison of the trajectories of 65 and 70 μm droplets.

The remainder of the experimental investigation was carried out under constant atomization conditions, using an atomizing air pressure of 44.6 N/cm^2 and a feed temperature of 285 K. Thus a D_{vs} of 26 μm and a constant drop size distribution were used in all tests, except those where the feed temperature was the variable studied.

Effect of inlet air temperature

The inlet air temperature was varied at a constant mass flow rate of drying air (corresponding to 8.72 m^3/min of free air measured at 294 K and 10^5 N/m^2 and a fixed nozzle

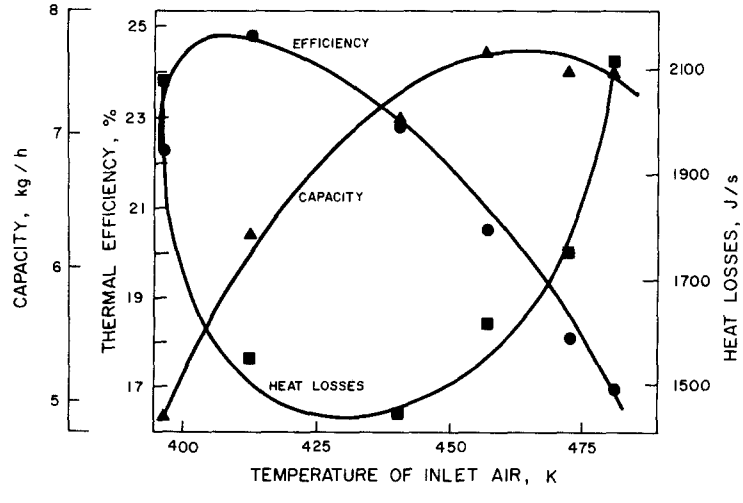

Figure 6. Effects of increasing inlet air temperature on chamber capacity, efficiency and heat losses.

* Detailed tables of results have been deposited as Document No. 1725 with the National Auxiliary Publications Service (NAPS), c/o Microfiche Publications, 305 E. 46th Street, New York, N.Y. 10017 and may be obtained for $1.50 for microfiche or $2.00 for photocopies.

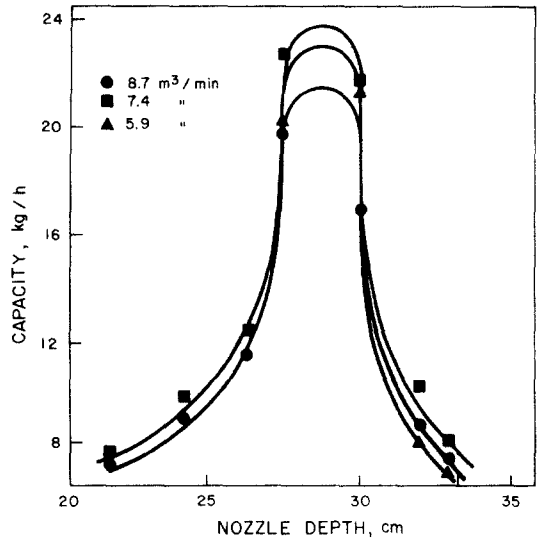

Figure 7. Effects of nozzle position and inlet air rate on chamber capacity.

depth of 32.7 cm below the roof of the chamber. The effects on capacity, efficiency and heat losses are shown in figure 6. The latter indicates that both capacity and efficiency pass through a maximum with increased inlet air temperature, but the two maxima do not occur at the same temperature. The curve for heat losses passes through a minimum at a point in the region of maximum efficiency.

As the inlet air temperature increases, both the rate of heat transfer to the droplets and the latter's velocity increase. The former effect predominates until an optimum temperature of 456 K is reached. Beyond this temperature, the capacity begins to decrease, owing to a shorter droplet path and higher heat losses.

Effect of nozzle position and inlet air rate

The effects of varying the rate of inlet air (measured as free air at 294 K and $10^5 N/m^2$) and the nozzle depth from the top of the chamber, at a constant inlet gas temperature of 456 K are shown in figure 7. The latter clearly demonstrates the importance of the nozzle location on the chamber capacity and the existence of a sharply defined optimum position between depths of 27.31 and 29.85 cm. More striking still is the fact that this optimum position appears to be independent of the inlet air rate. For all nozzle positions, there exists an optimum air rate (7.42 m^3/min) which appears to be the same in all cases.

Additional results not shown here indicate that at maximum capacity the efficiency is also maximum and the heat losses are minimum, as a function of nozzle position. However, the optimum values do not occur at the same air flow rates. That higher efficiencies should be attained at lower rates was to be expected, because of the longer residence times available for evaporation. In other words, it can be predicted that increased efficiency should result

when equal capacities are attained at lower rates of drying air. This was experimentally confirmed when an optimum thermal efficiency of 92% was recorded for 4.98 m^3/min (capacity = 20.1 kg/h) as compared with 71% for 5.89 m^3/min (capacity = 21.2 kg/h).

Effect of air temperature at optimum nozzle depth

Keeping the nozzle depth constant at the optimum value of 27.3 cm previously found, it was decided to re-examine the effect of increased inlet air temperature. The inlet air rate was also kept constant at the optimum value of 7.42 m^3/min of free air (or at a constant mass rate of 499.4 kg/h). The effects on capacity and efficiency are shown in figure 8.

The results indicate that a maximum was again found for the capacity of the chamber although the variations in capacity were not large. This maximum did not correspond to a maximum efficiency nor to minimum heat losses. As a matter of fact, the heat losses increased rapidly with the air temperature, causing a corresponding sharp decrease in efficiency.

Effect of inlet feed temperature

The inlet temperature of the feed water was varied under operating conditions which had previously led to maximum capacity, namely an air rate of 7.42 m^3/min, a nozzle depth of 27.31 cm and an inlet air temperature of 489 K. The effects on capacity and efficiency are shown in figure 9. It is probable that the capacity reported for a feed temperature of 343 K is slightly too low. Lyons (1951) made a detailed study of this particular factor in the same experimental apparatus, and his results clearly indicated that the capacity remained approximately constant at higher feed temperatures. The capacity curve in figure 9 was

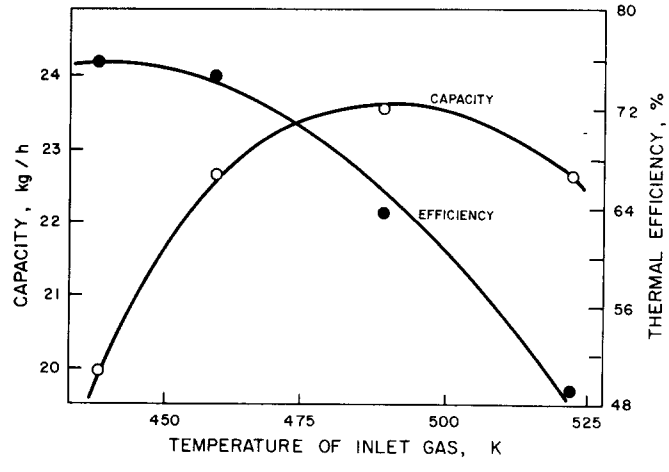

Figure 8. Effect of inlet air temperature at optimum nozzle depth on chamber capacity and efficiency.

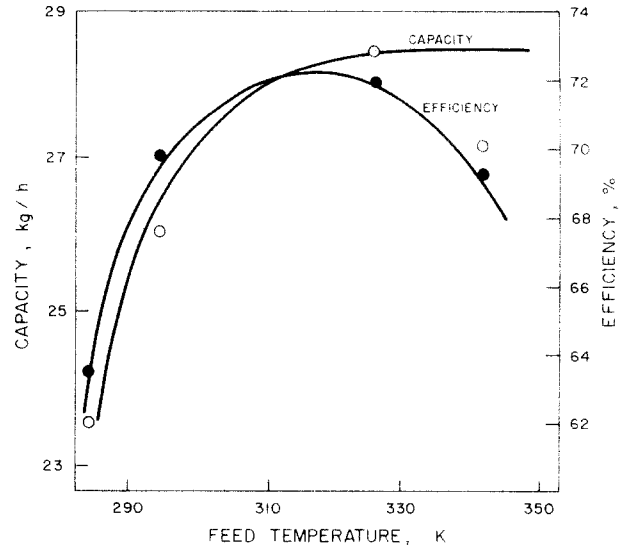

Figure 9. Effect of inlet feed temperature on chamber capacity and efficiency.

therefore drawn accordingly. Lyons confirmed that the efficiency curve passed through a maximum as observed in the present work, and then decreased slightly due to increased heat losses.

These results are particularly interesting because they show large effects on the capacity and efficiency which were totally unexpected. The capacity appears to reach a maximum at a temperature of the inlet feed corresponding to the wet-bulb temperature of the drying air (326 K). To account for this behaviour, it must be remembered that a marked cooling accompanies the expansion of the atomizing gas in a pneumatic nozzle. Increasing the feed temperature will overcome this detrimental factor to some extent. More important still is the decrease in D_{vs} (down to 24 μm at 326 K) and its accompanying decrease in the largest droplet size which results from higher feed temperatures.

CONCLUSIONS

In spite of its small size, the spray-drying chamber used in this study exhibited many of the operating characteristics displayed by its much larger industrial counterparts with, however, one important exception, namely the large evaporative capacity of the nozzle zone as compared with that of the free-entrainment zone. In an industrial spray dryer the opposite behaviour would be observed. This explains the large influence exerted by the feed temperature on the capacity of the chamber, as shown in figure 9. This effect would undoubtedly be less pronounced in a large chamber. In all other respects the trends reported in this study should hold, irrespective of the chamber size.

An important limitation to this work is that no effort was made to optimize the design of the air inlets. From the work of Schowalter & Johnstone (1960) and the qualitative observations of Marshall (1954), it can be inferred that the entrance conditions used in this

study induced the drying air to assume a spiral motion with a pronounced downward pitch, with probably less than a full turn before reaching the conical section of the chamber. Unfortunately, this assumption cannot be experimentally verified, since the exact path of the air was not ascertained, at least in the upper part of the chamber.

Another interesting point to be noted is that the end of the nozzle zone (at which point the unevaporated droplets begin to be entrained by the swirling drying gas) was located about 104 cm below the roof of the chamber for the optimum nozzle position. This is well within the conical section. It can therefore be inferred that the top part of the chamber was largely inoperative in the drying process. On the other hand, the maximum thermal efficiency observed was 92% (t_1 = 458 K, 4.98 m^3/min) indicating that under the operating conditions used, the drying capacity of the air was almost fully utilized, in spite of the fact that the contact time between droplets and drying gas was limited to a short period in the conical section. This leads to the conclusion that, for efficient operation, it is not necessary that droplets and drying gas be in contact during the whole residence time of the *latter* through the chamber. It is only necessary that mass and heat transfer be adequate during the time they are in contact. This of course underlines the importance of the path length and residence time of the droplet when in contact with the gas.

The major contribution of this work was to establish that it is now possible to calculate solely from theoretical considerations and with reasonable accuracy the momentum, heat and mass transfer to droplets in both the nozzle zone and the entrainment zone of a spray-drying chamber. In the nozzle zone, the calculations agreed with the observed length of the spray (~76 cm) and its angle of spread (~22°). Admittedly, the calculations were based on initial values of drop velocities experimentally reported by Manning & Gauvin (1960) for an identical atomizing nozzle. This information, together with the droplet size distribution and the size of the largest droplet should in the future be supplied by the manufacturer of the nozzle as part of the latter's specifications. It may even be possible, in time, to predict these nozzle characteristics from theoretical considerations.

Calculations of the droplet path in the free-entrainment zone were again in reasonable agreement with the experimental evidence. In the case of the example discussed in Section 1, they indicated that, for the conditions used, the rate of heat and mass transfer were adequate to completely vaporize the largest (65 μm) droplet before it could reach the wall in the contact path available. Had this droplet been initially slightly larger (70 μm), the contact path would not have been sufficient, as shown in figure 3.

It is now relatively simple to interpret the effects on the capacity and thermal efficiency of each of the operating conditions studied (drying air temperature and mass flow rate, nozzle position and feed temperature) in terms of the droplet trajectories in each case. In general, capacity will increase as the heat and mass transfer rates increase and as the droplet residence time increases. Efficiency will be similarly influenced, but in addition it is affected by heat losses.

The most interesting aspect of this study is probably the marked influence on capacity exerted by the nozzle position, as shown in figure 7. Remembering the work of Schowalter & Johnstone (1960), it is not surprising that the nozzle optimum position is independent of the gas flow rate, since these authors have shown that the mean flow pattern of the gas was

unaffected by the latter. A similar observation had been reported earlier by Eckert & Hartnett (1955). As a matter of fact, it can be inferred that the mean flow pattern of the drying air did not change appreciably throughout this study, although its temperature and velocity of course did. Moreover, its spiral motion had very likely a very pronounced downward pitch in the cylindrical and upper part of the conical section, although it probably became much tighter in the bottom part of the latter. This assumption is borne out at least qualitatively, by the rapid decrease in V_t shown on figure 2 in the early stages of the droplet's residence time.

That the optimum capacity on figure 7 for a given nozzle depth should occur at an intermediate flow rate of the gas can be explained by the fact that at high flow rates, the high droplet velocity limits its residence time, while at low gas flow rates, the drying capacity of the entering gas is simply too low. It should be noted, however, that the highest efficiencies reported in this work were obtained under the latter conditions.

It has been mentioned that the turbulence characteristics of the flow were not measured in this work. As previously noted, the turbulence intensity can reach fairly large values, particularly in the atomized jet and near the axis of the chamber in the free-entrainment zone. However, the Reynolds numbers of the droplets are, on the average, so small as to make the effect of the turbulence intensity on the heat and mass transfer rates almost negligible, as observed by Dlouhy & Gauvin (1960). The effect of Spalding number in the present study has been estimated to be negligible.

The values of the drag coefficient used in the present calculations may not be strictly valid when used in connection with the tangential and radial motions of the droplets. It is hoped, that in the future, investigations will be carried out to elucidate this point. It is of interest to note that Sivier (1967) observed no significant change in C_D for $Re < 200$ in the turbulence intensity range of about 1–8 %.

Although water was used as the feed material for convenience in this study, it is evident that the same analytical and computational approach can be used in the case of an actual solution, with minor modifications. Work on the drying of an organic product has been carried out in this laboratory and the results will be presented in a subsequent paper.

NOMENCLATURE

A, B, C_1, C_2	constants
A_p	projected area of droplet on a plane normal to mean flow, m^2
C_D	drag coefficient
C_p	heat capacity, J/kg. K
C_{s1}, C_{s2}	heat capacity of inlet and outlet humid air, J/kg. K
D	diameter of largest droplet, μm
D_i	diameter of each class of droplets, μm
D_0	diameter of nozzle, cm
D_{vs}	Sauter mean diameter, $\sum n_i D_i^3 / \sum n_i D_i^2$, μm
E	rate of evaporation, kg/h
F_L	lift force, N
g	acceleration due to gravity, m/s^2
h	heat transfer coefficient, $J/m^2.s.K$
H_1, H_2	absolute humidities of entering and leaving air, respectively, g of water vapor/g of dry air.
k_a	thermal conductivity of air, J/m.s.k
K	curl of fluid velocity, s^{-1}

m	mass of droplet, kg
M_e	mass flowrate of entrainment, kg/h
M_0	mass flowrate of atomizing air, kg/h
n_i	number of each class of droplets
q	rate of heat transfer to droplets, J/s
q_L	rate of heat losses from spray chamber, J/s
q_{Lz}	rate of heat losses up to point z, J/s
r	radial position of droplet, cm
R	radius of chamber at any height, cm
r_5	velocity half-radius, cm
t	time, s
t_a	temperature of drying air, K
t_d	datum temperature, K
t_f	feed temperature, K
t_w	wet bulb temperature of drying air, K
t_s	adiabatic saturation temperature, K
V_{at}, V_{ar}, V_{av}	absolute values of tangential, radial and axial velocities of air, respectively, m/s
V_c	velocity of air on the centerline of atomizing jet, m/s
V_f	resultant velocity of droplet relative to fluid, m/s
V_0	velocity of air at nozzle exit, m/s
V_t, V_r, V_v	absolute values of tangential, radial and axial velocities of droplet, respectively, m/s
V_{rel}	relative velocity between the gas and liquid streams at the nozzle exit, m/s
W_a	flowrate of atomizing air, kg/h
W_G	flowrate of drying air; (free air) kg of drying air/h
W_L	flowrate of feed, kg/h
$\bar{x}$	dimensionless distance, defined by equation [3]
x	vertical distance from nozzle, cm
z	position along droplet path

Greek letters

α, β	constants
Δ	increment
η	drying thermal efficiency, defined by equation [34]
θ	angular position of droplet, radians
λ_d	latent heat of vaporization at t_d, J/kg
λ_w	latent heat of vaporization at t_w, J/kg
μ_a	viscosity of air, N.s/m^2
ν	kinematic viscosity of air, m^2/s
ρ_a	density of air, kg/m^3
ρ_a	density of the surroundings of the jet, kg/m^3
ρ	density of droplet, kg/m^3
ω	angular velocity of droplet, rad/s

Dimensional groups

Nu	Nusselt number, hD/k_a
Pr	Prandtl number, $C_p\mu_a/k_a$
Re	Reynolds number, $DV_f\rho_a/\mu_a$
B	Spalding number, $C_p\Delta T/\lambda_w$

Subscripts

1	at the inlet conditions of spray dryer
2	at the outlet conditions of spray dryer
a	of air
d	at datum temperature
0	at nozzle exit
x	at a vartical distance x below the nozzle
w	at wet bulb temperature of the air
z	at a position z along the droplet path

REFERENCES

ABRAMOVICH, G. N. 1963 The Theory of Turbulent Jets, pp. 586–598. M.I.T. Press.

ALBERTSON, M. L., DAI, Y. B., JENSON, R. A. & ROUSE, H. 1950, Diffusion of submerged jets. *ASCE Trans.* **115**, 639–697.

BAILEY, G. H., SLATER, I. W. & EISENKLAM, P. 1970 Dynamic equations and solutions for particles undergoing mass transfer. *Br. Chem. Engng* **15**, 912–916.

BALTAS, L. & GAUVIN, W. H. 1969a Performance predictions for a current spray dryer. *A.I.Ch.E.J.* **15**, 764–71.

BALTAS, L. & GAUVIN, W. H. 1969b Transport characteristics of a concurrent spray dryer. *A.I.Ch.E.J.* **15**, 772–779.

BEARD, K. V. & PRUPPACHER, H. R. 1969 A determination of the terminal velocity and drag of small water drops by means of a wind tunnel. *J. Atmos. Sci.* **26**, 1066–1072.

BECKER, H. A., HOTTEL, H. C. & WILLIAMS, G. C. 1963 Mixing and Flow in Ducted Turbulent Jets, *Ninth Int. Symp. Combustion*, pp. 7–20. Academic Press.

DAVIES, J. T. 1972 *Turbulence Phenomena* pp. 98–99, Academic Press.

DLOUHY, J. & GAUVIN, W. H. 1960 Evaporation rates in spray drying. *Can. J. Chem. Engng* **38**, 113–120.

ECKERT, E. R. G. & HARTNETT, J. P. 1955 Experimental Study of Velocity and Temperature Distribution in High Velocity Vortex Type Flow. Univ. Minn. Heat Transfer Lab. Tech. Report No. 6.

ECKERT, E. R. G. & HARTNETT, J. P. 1956 Experimental Study of Velocity and Temperature Distribution in High Velocity Vortex Type Flow, Heat Transfer and Fluid Mechanics Institute, pp. 135–150, Stanford University Press.

EDELING, C. 1949 *Beihefte Angew. Chem.* **57**, 1–54.

GAL, G. 1970 Self-preservation in fully expanded turbulent coflowing jets. *AIAA J.* **8**, 814–815.

GAUNTNER, J. W., LIVINGHOOD, J. N. B. & HRYCAK, P. 1970 Survey of Literature on Flow Characteristics of a Single Turbulent Jet Impinging on a Flat Plate. NASA TN D-5652.

HILSENRATH, J., BECKETT, C. W., BENEDICT, W. S., FANO, L., HOGE, H. J., MASI, J. F., NUTTAL, R. L., TOULOUKIAN, Y. S. & WOOLLEY, H. W. 1955 Tables of Thermal Properties of Gases. Nat. Bur. Standards Circular No. 564.

HINZE, J. O. 1959 *Turbulence*, pp. 354–355. McGraw-Hill.

HOFFMAN, T. W. & ROSS, L. L. 1972 A theoretical investigation of the effect of mass transfer on heat transfer to an evaporating droplet. *Int. J. Heat Mass Transfer* **15**, 599–617.

KIM, K. Y. & MARSHALL, W. R., Jr. 1971 Drop size distributions from pneumatic atomizers. *A.I.Ch.E.J.* **17**, 575–584.

LAWLER, M. T. & LU, P. C. 1970 The role of lift in the radial migration of particles in a pipe flow, *Advances in Solid–Liquid Flow in Pipes and its Application* (Edited by IRAJ ZANDI), pp. 39–57. Pergamon Press.

LEWELLEN, W. S. 1971 A Review of Confined Vortex Flows, N71–32276. M.I.T. Press.

LYONS, D. B. 1951 The Effects of Feed Properties on Spray Drying. M.Eng. Thesis, McGill University, Montreal.

MANNING, W. P. & GAUVIN, W. H. 1960 Heat and mass transfer to decelerating finely atomized sprays. *A.I.Ch.E.J.* **6**, 184–90.

MARSHALL, W. R., Jr. 1954 *Atomization and Spray Drying*, Chem. Engng Prog. Monograph Series, No. 2, Vol. 50, pp. 102–103.

MASTERS, K. 1972 *Spray Drying*. Leonard Hill.

PAL, S. 1954 *Fluid Dynamics of Jets*, p. 120. Van Nostrand.

PITA, E. G. 1969 Heat and Mass Transfer in Evaporating Sprays. Ph.D. Thesis, University of Maryland, College Park, Maryland.

PLACE, G., RIDGEWAY, K. & DANCKWERTS, P. P. 1959 Investigation of air-flow in a spray dryer by tracer and model techniques. *Trans. Inst. Chem. Engrs* **37**, 268–276.

RANZ, W. E. & MARSHALL, W. R. 1952 Evaporation from drops—Part I & Part II. *Chem. Engng Progr.* **48**, 141–146; 173–180.

SAFFMAN, P. G. 1965 The lift on a small sphere in a slow shear flow. *J. Fluid Mech.* **22**, 385–400.

SCHOWALTER, W. R. & JOHNSTONE, H. F. 1960 Characteristics of the mean flow patterns and structure of turbulence in spiral gas streams. *A.I.Ch.E.J.* **6**, 648–655.

SIVIER, K. R. 1967 Subsonic sphere drag measurements at intermediate Reynolds numbers. Ph.D. Thesis, University of Michigan.

Résumé—Pour le calcul des sécheurs à brouillard, la connaissance des trajectoires des gouttelettes atomisées est nécessaire, à la fois dans la zône de l'ajutage (où les gouttelettes décèlèrent rapidement à partir d'une vitesse initiale élevée) et dans la zône d'entrainement libre (où les gouttelettes sont transportées par le gaz sécheur), car elle gouverne la capacité d'évaporation et le rendement thermique de l'enceinte, tout en affectant le taux d'humidité et la qualité du produit par l'intermédaire due temps de séchage.

On a déterminé théoriquement, dans les deux zônes, les trajectoires des gouttelettes en mouvement tridimensionnel. Dans le cas des atomiseurs pneumatiques à deux fluides, on a trouvé que les caractéristiques du jet de fluide atomiseur sont importantes dans les deux zônes.

La prévision des trajectoires de gouttelettes a été contrôlée avec une chambre de séchage expérimentale à co-courant, circulaire à fond conique, et dans laquelle l'air de séchage était introduit tangentiellement près du haut. On a utilisé de l'eau pour l'alimentation de l'appareil. On a étudié les influences des débits et des températures de l'eau et de l'air, et celle de la position de l'injecteur, sur le rendement thermique et la capacité d'évaporation de la chambre. On a interprété les résultats à la lumière des trajectoires calculées pour les gouttelettes.

Auszug—Eine Kenntnis der Bahnen der zerstaeubten Tropfen, sowohl in der Deusenzone (wo die Tropfen schnell von ihrer hohen Anfangsgeschwindigkeit verzoegert werden), wie auch in der Zone freien Mitreissens (in der die Tropfen durch das Trockengas mitgefuehrt werden), ist fuer den Entwurf von Zerstaeubungstrocknern erforderlich. Sie bestimmen die Verdampfungsleistung und den thermischen Wirkungsgrad der Trockenkammer, wie auch, durch ihren Einfluss auf die Trockenzeit, den Feuchtigkeitsgehalt und die allgemeine Guete des Erzeugnisses. Die Tropfenbahnen der dreidimensionalen Bewegung in beiden Zonen wurden theoretisch bestimmt. Im Fall von pneumatischen Zweistoff-Fluessigkeitszerstaeubern wurde gefunden, dass die Eigenschaften des Zerstaeuberstrahles in beiden Zonen von Wichtigkeit sind. Voraussagen von Tropfenbahnen wurden in einem im Gleichstrom betriebenen kreisfoermigen Zerstaeubungstrockner mit konischem Boden experimentell nachgeprueft. Die Trockenluft wurde am oberen Ende tangential eingefehrt; zur Beschickung wurde Wasser verwandt. Der Einfluss der folgenden Faktoren auf die Verdampfungsleistung und den thermischen Wirkungsgrad wurde untersucht: Durchsatz und Temperatur der Fluessigkeit, Trockenluftmenge und -temperatur, und die Duesenanordnung. Die Ergebnisse wurden anhand der voraussesagten Tropfenbahnen gedeutet.

Резюме—Знание траекторий распъленных капелек как в зоне сопла (где эти капелък быстро замедляютсн со своей высокой началъной скорости), так и в зоне свободного затопления струи (где канолъюи транспортируются осушающим газом) необходимо для просктиро вания распыляющих осушителей, посколъку оно определяэт испаряющую способностъ и тепловой коэффициент нолезного действия камеры, в то время как содержание вцаги и общсе юл состояние продукта учитываетсн изменением времени осушения.

Траектории капелек в трех измерениях были оцределены в обеих зонах теоретически. Характеристики факела распълекно жидкости для двухжидкостного пневматического распылителя, как найдено, являютсо важными для обеих зон.

Предсказанные траектории капелек бнли проверены в экспериментальяой круговой прямоточной распыляющей сушилъной камере с коническим дном, вблизи потолка которой тангенциалъно вводился осушающий воздух, а в качестве транспортирующей среды и сполъзоваласъ вода. Были изучены влияние скорости подачи жидкости и ее температуры, скорости потока осушающего воздуха и его температуры, а также влияние положения содла на тепловой коэффициент полезного действия и осушающую способностъ камеры. Резлкътаты представлены в свете предсказанных траекторий капслек.